Supporting information

Mo-doped PdCu Nanoparticles as High-Performance Catalysts for Oxygen Reduction Reaction

Kailu Kang, [a] Xing Hu, [a] Pei Zhang, [a] Yangyang Zhang, [a] Shan Zhu, [a] Kaixiang Lei, [a] Kezhu Jiang*[a] and Shijian Zheng*[a b]

[a] Technology, School of Materials Science and Engineering, Hebei University of Technology.

Tianjin 300401, China

[b] Tianjin Key Laboratory of Materials Laminating Fabrication and Interface Control

Technology. Tianjin 300401, China
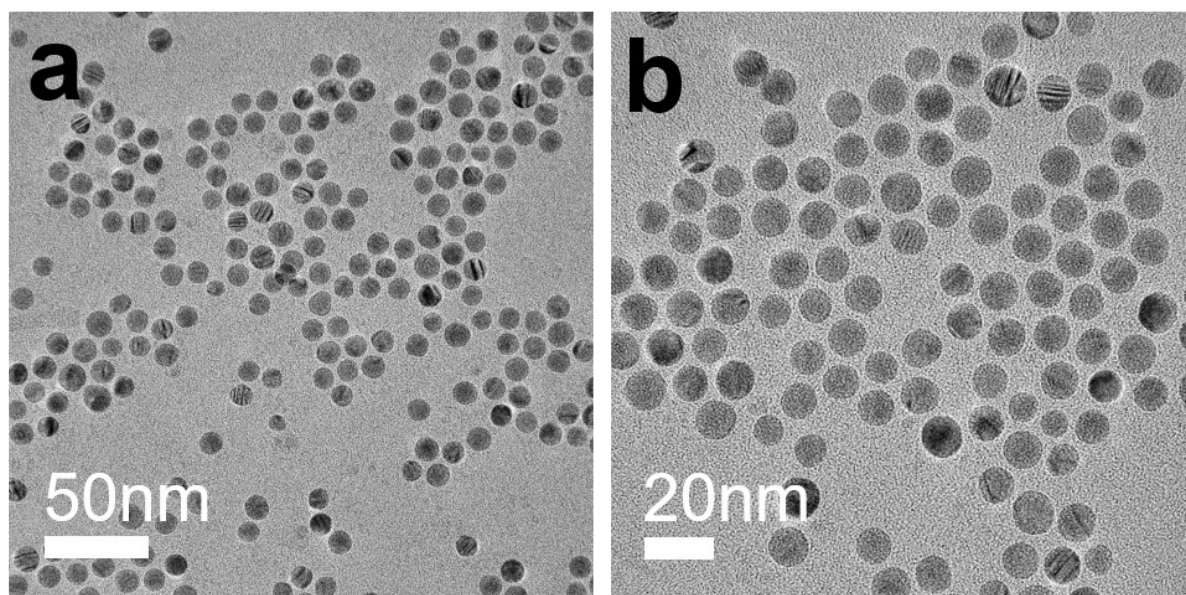
1: Supplementary Figures

Figure S1. TEM images of Mo-PdCu-1 NPs. (a) low-magnification TEM image and (b) high-magnification TEM image of Mo-PdCu-1 NPs.
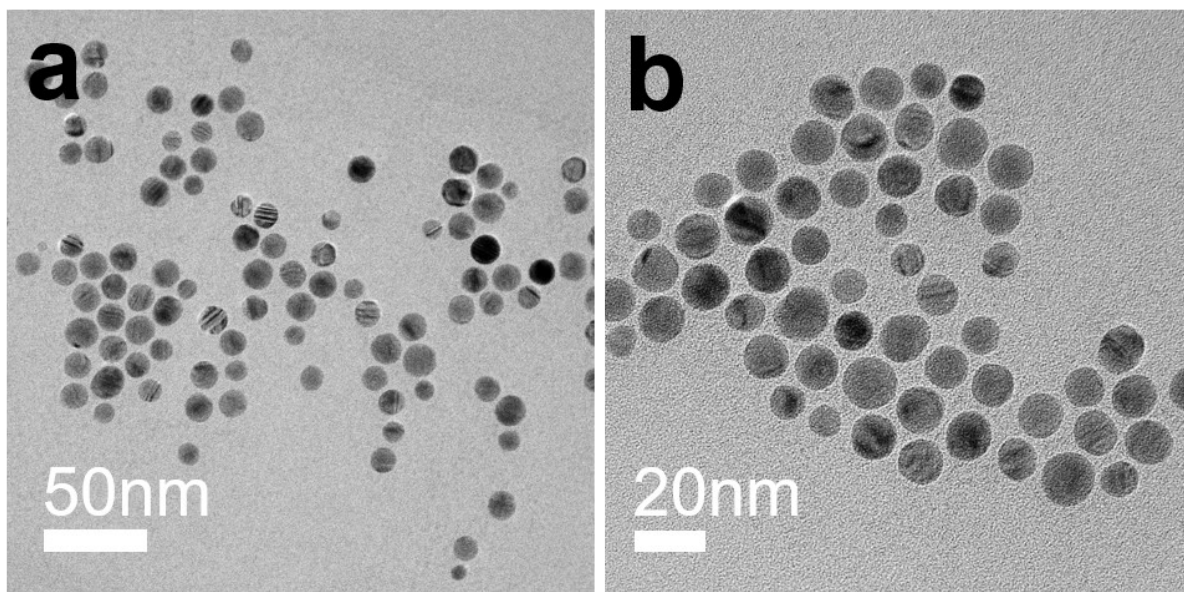
Figure S2. TEM images of Mo-PdCu-2 NPs. (a) low-magnification TEM and (b) high-magnification TEM images of Mo-PdCu-2 NPs.
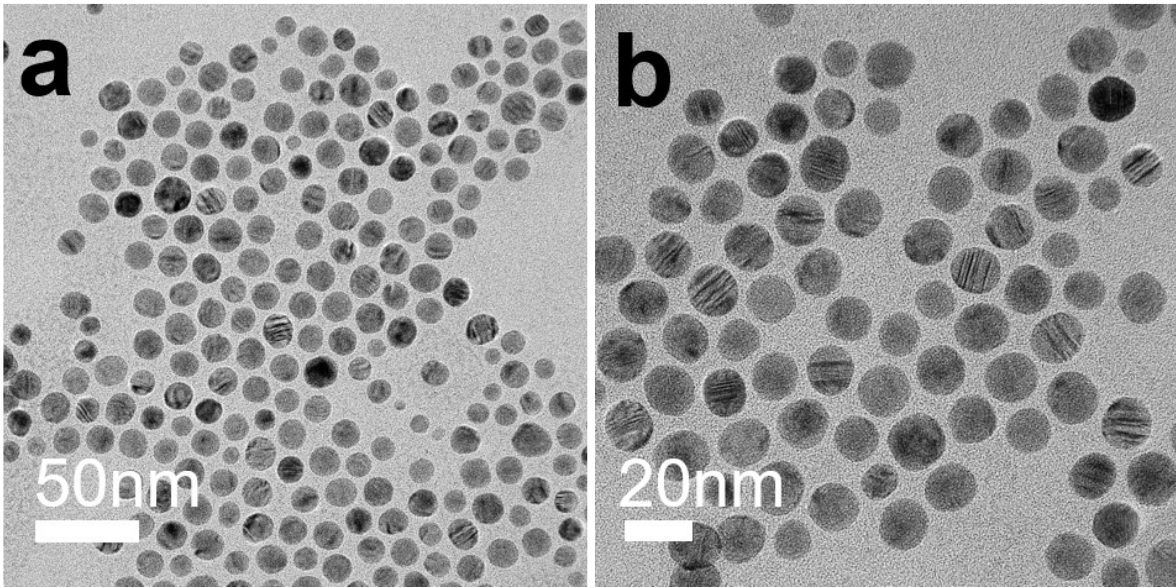
Figure S3. TEM images of Mo-PdCu-3 NPs. (a) low-magnification and (b) high-magnification TEM images of Mo-PdCu-3 NPs.
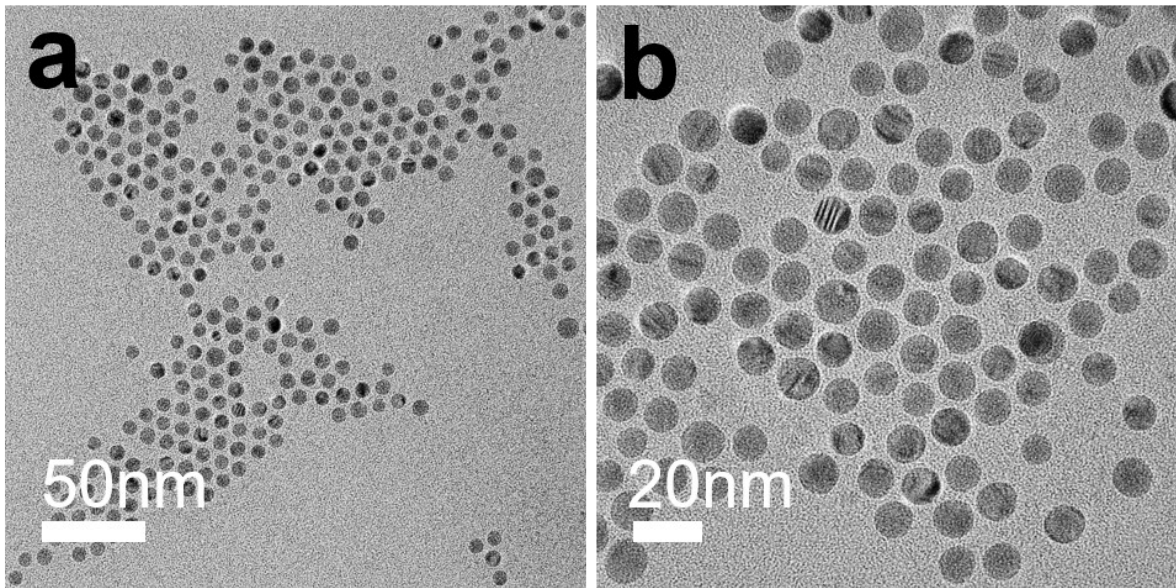
Figure S4. TEM images of PdCu NPs. (a) low-magnification TEM image, (b) high-magnification TEM image and (c)XRD pattern of PdCu NPs.
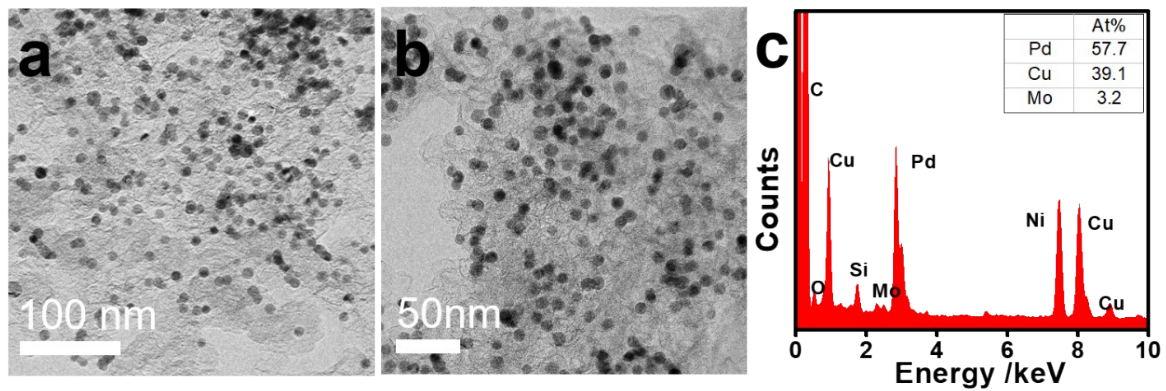
	At%
Pd	57.7
Cu	39.1
Mo	3.2

Figure S5. The morphology and composition characterization of Mo-PdCu-1/C. (a, b) TEM images and (c) STEM EDS pattern of Mo-PdCu-1/C.
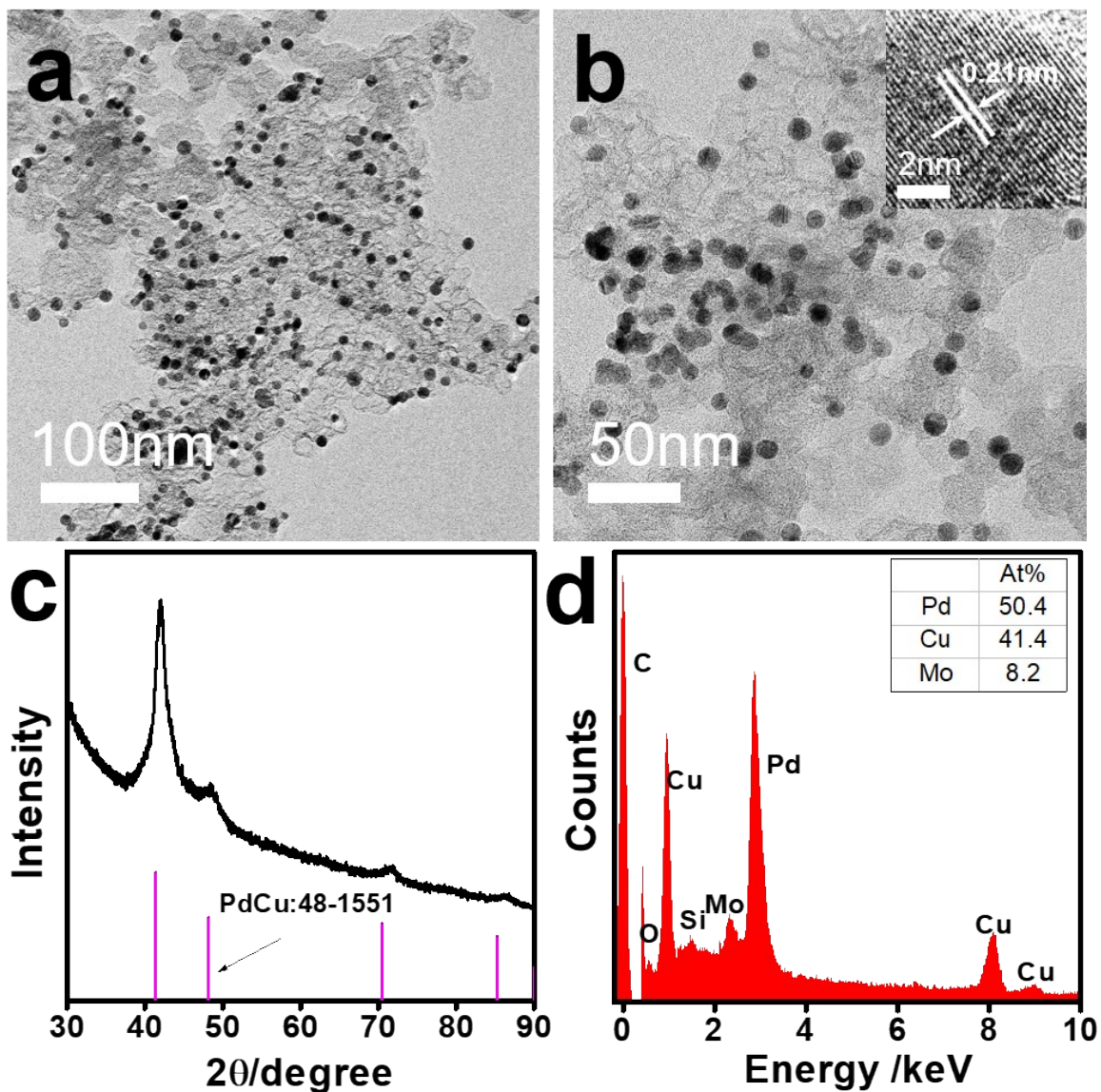
Figure S6. The morphology, composition and structure characterization of Mo-PdCu-2/C. (a, b) TEM images, (c) XRD pattern and (d) SEM-EDS pattern of Mo-PdCu-2/C. The inset: HRTEM image of Mo-PdCu-2/C.
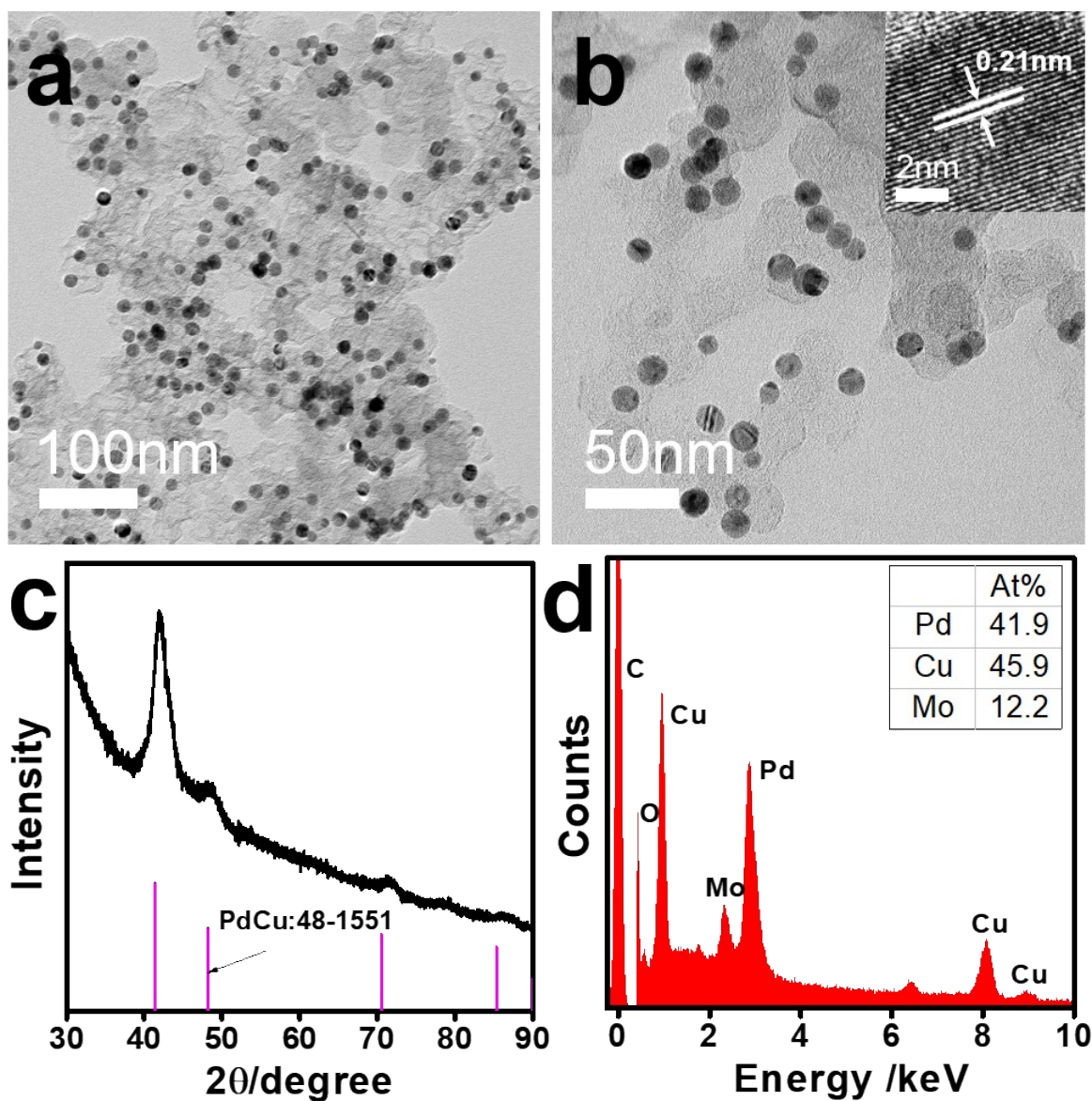
Figure S7. The morphology, composition and structure characterization of Mo-PdCu-3/C. (a, b) TEM images, (c) XRD pattern and (d) SEM-EDS pattern of Mo-PdCu-3/C. The inset: HRTEM image of Mo-PdCu-3/C.
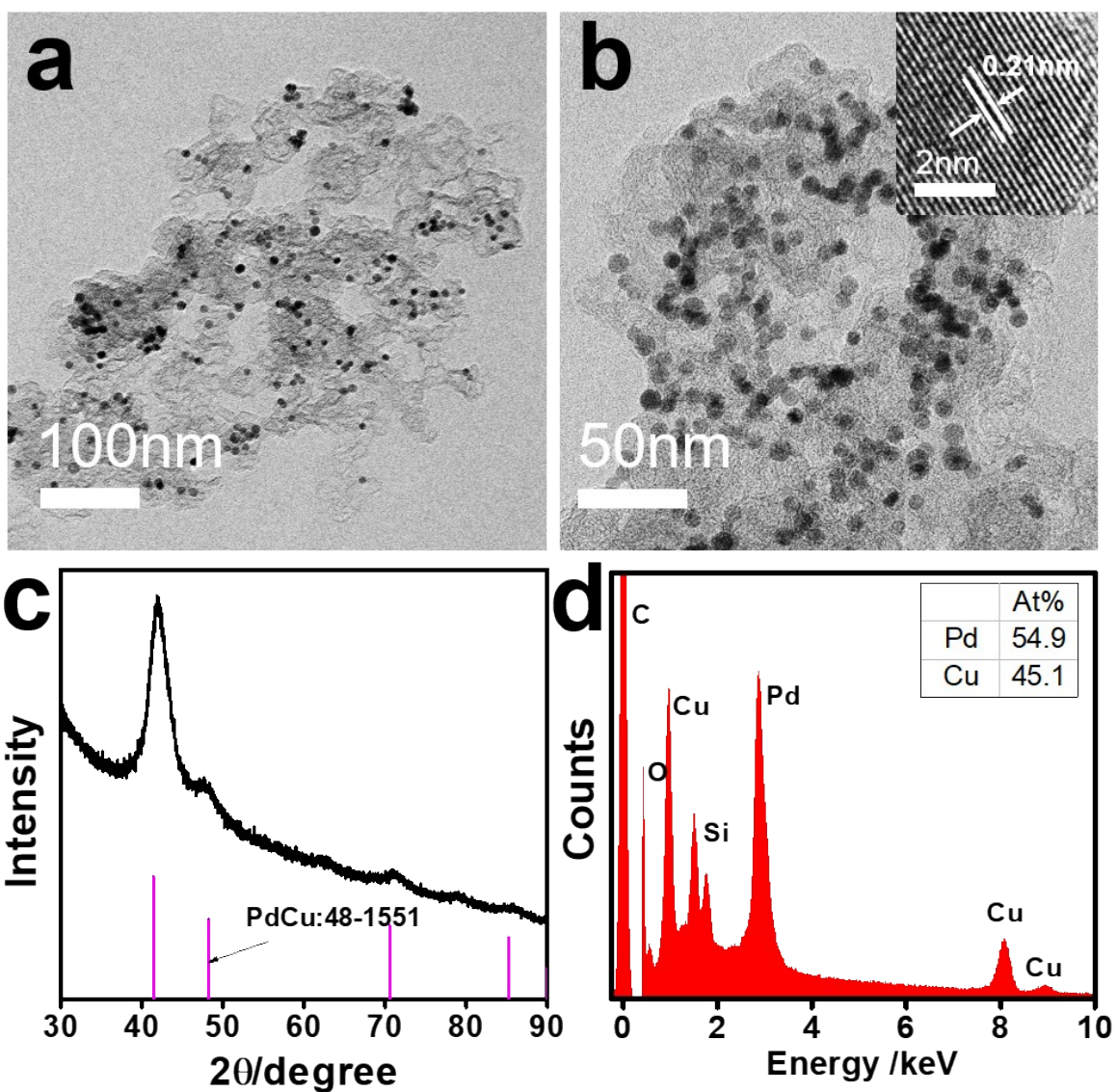
Figure S8. The morphology, composition and structure characterization of PdCu/C. (a, b) TEM images, (c) XRD pattern and (d) SEM-EDS pattern of PdCu/C. The inset: HRTEM image of PdCu/C.
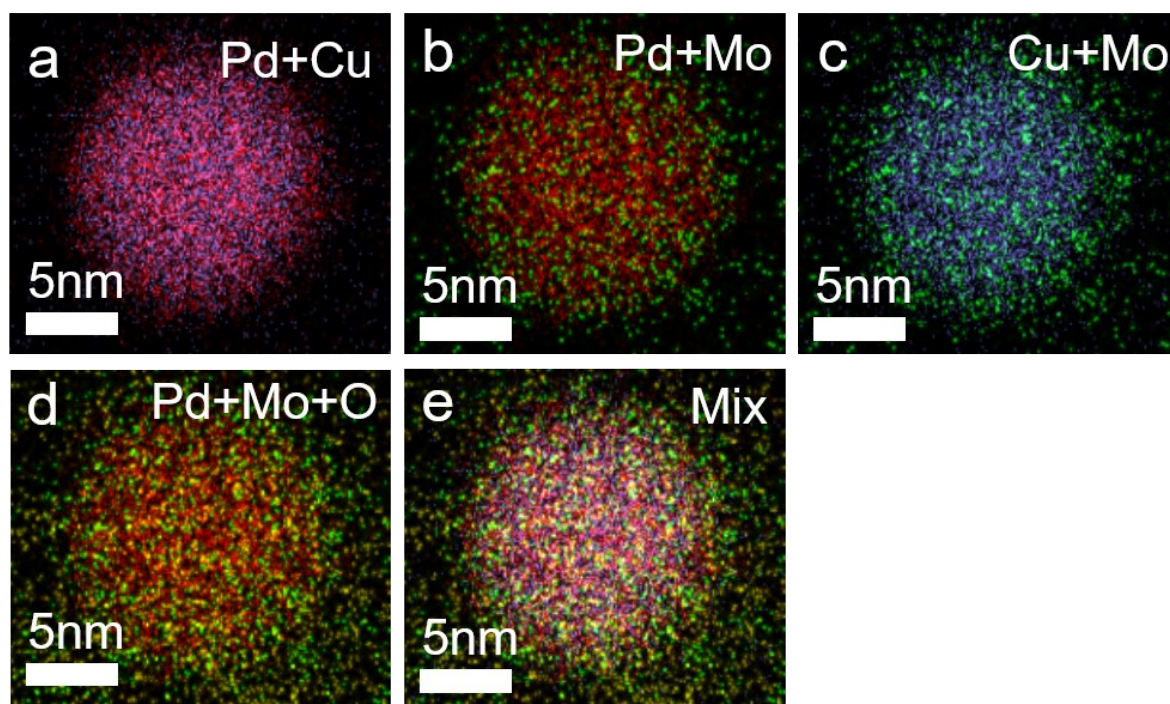
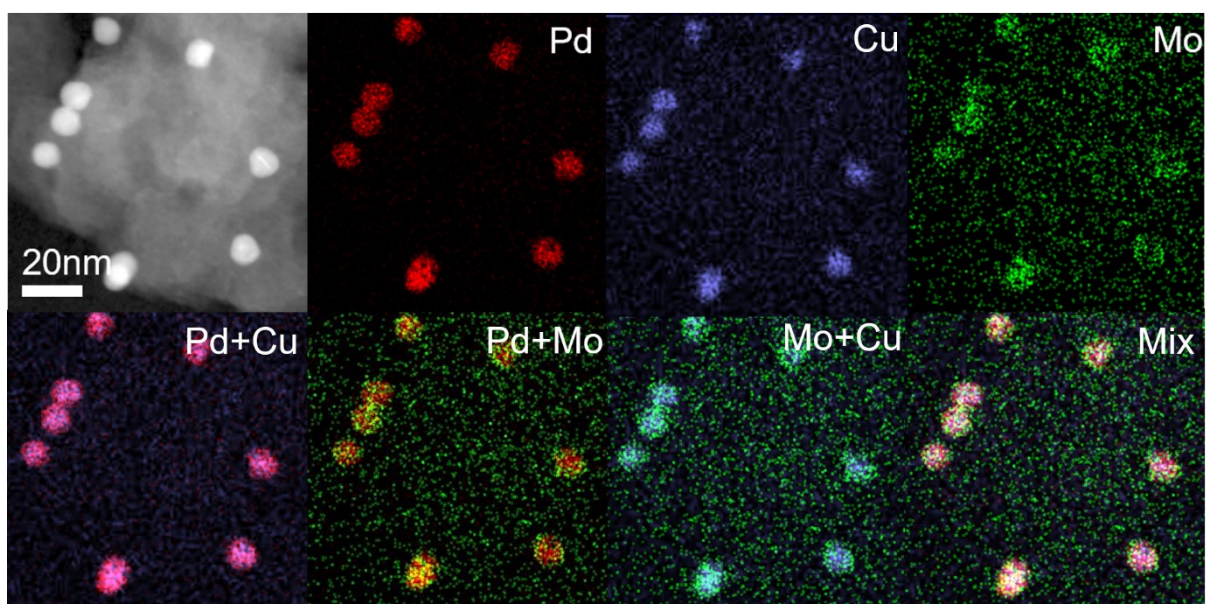**Figure S9.** HAADF-STEM-EDS elemental mapping images of single Mo-PdCu-1/C.

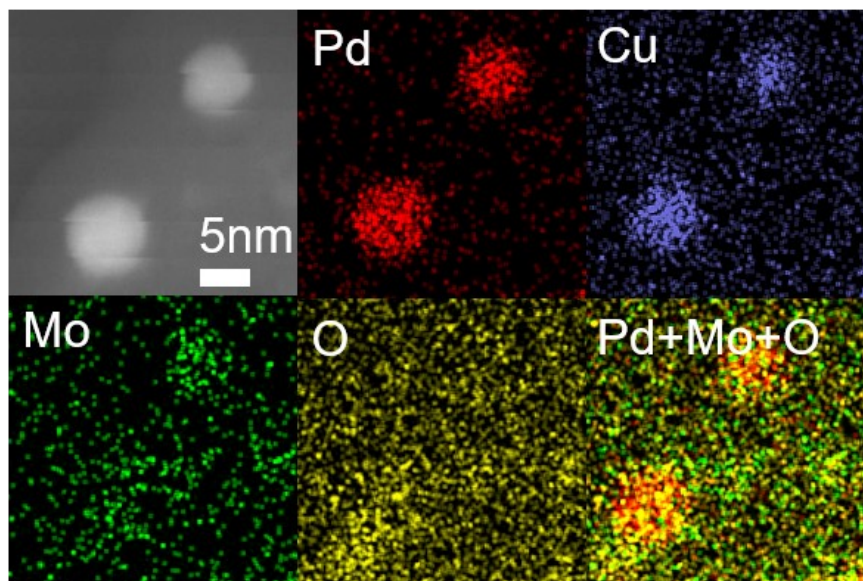**Figure S10.** HAADF-STEM-EDS elemental mapping images of Mo-PdCu-1/C.

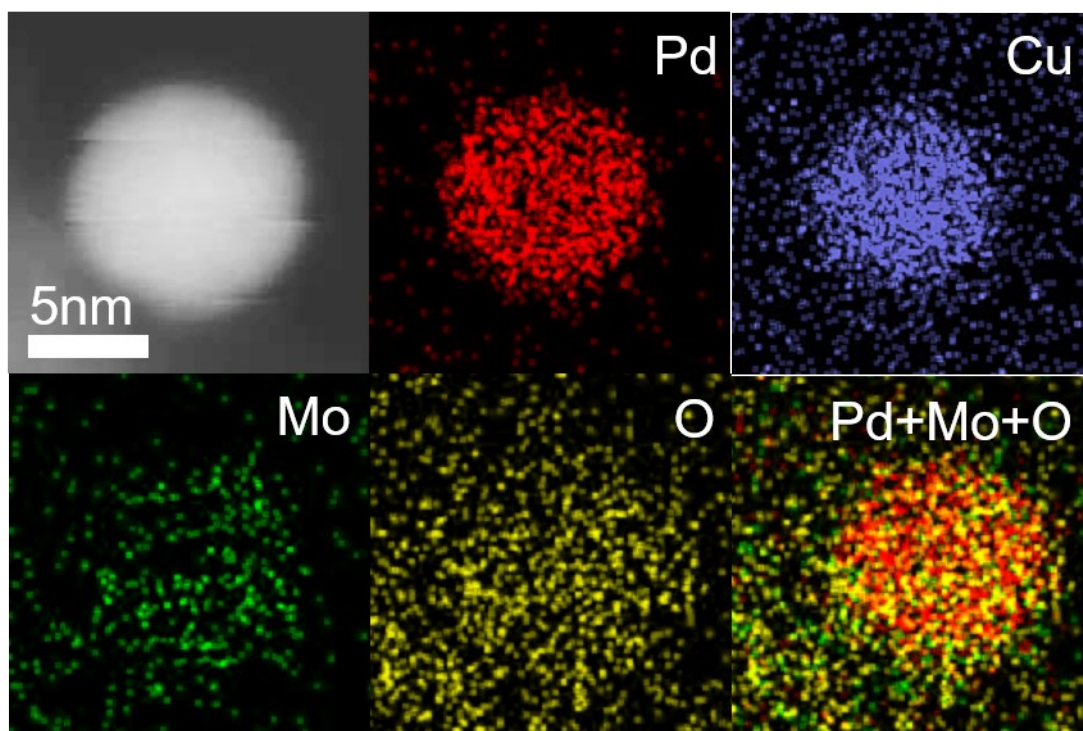**Figure S11.** HAADF-STEM-EDS elemental mapping images of Mo-PdCu-2/C.

Figure S12. HAADF-STEM-EDS elemental mapping images of Mo-PdCu-3/C.

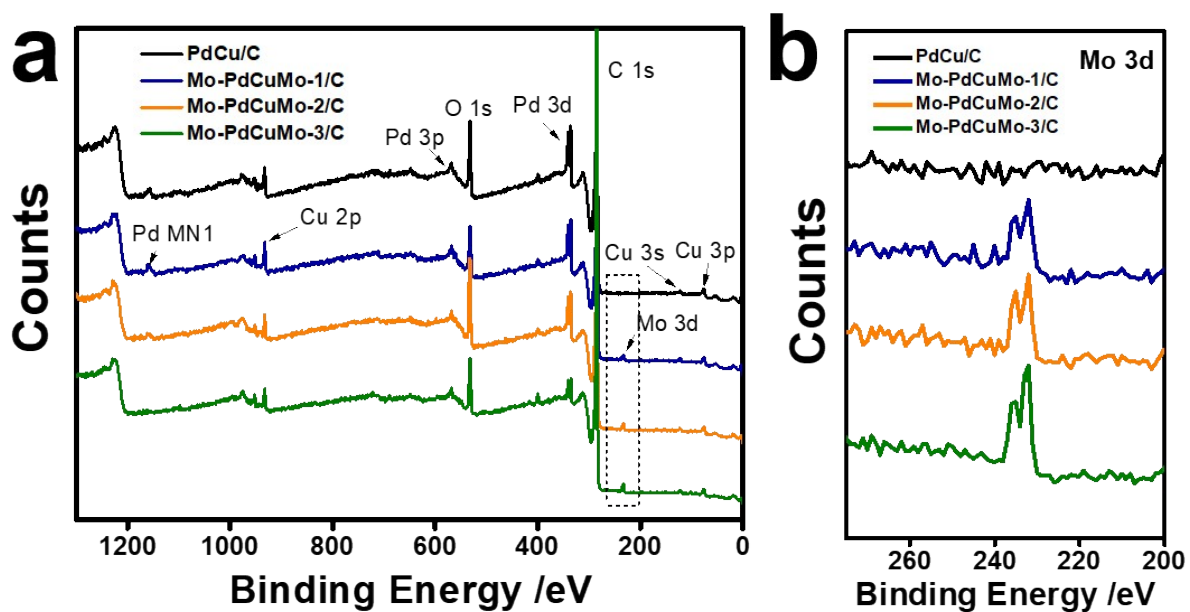**Figure S13.** XPS spectra of the catalysts. (a) XPS whole pattern of PdCu/C, Mo-PdCu-1/C, Mo-PdCu-2/C, Mo-PdCu-3/C. (b) Partially enlarged pattern of (a).
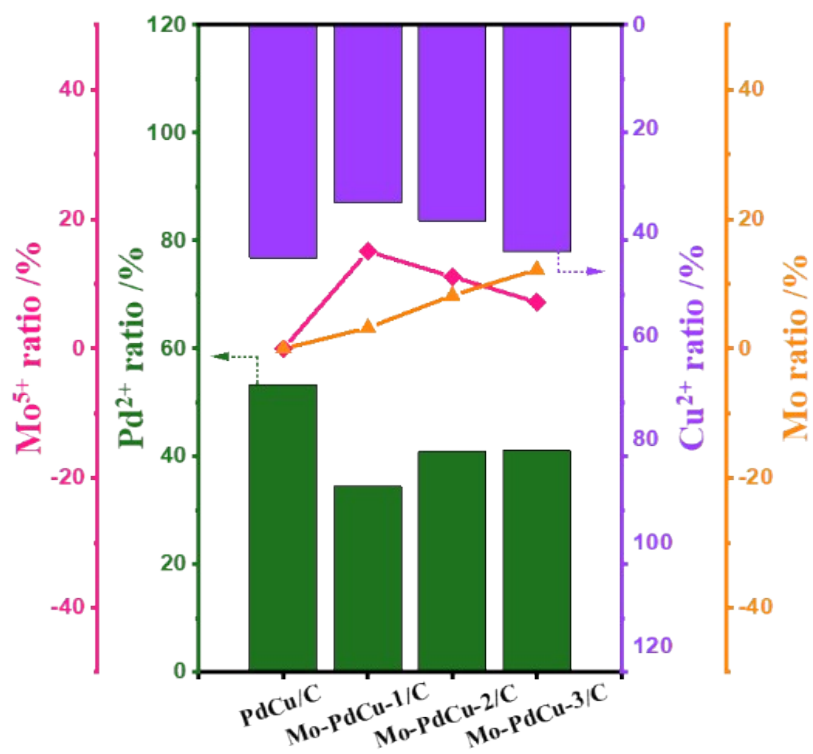
Figure S14. The ratio change of Mo, Mo^{5+}, $Pd^{2+,}$ and Cu^{2+} from XPS. Among them, Mo, Mo^{5+}, $Pd^{2+,}$ and Cu^{2+} correspond to orange, pink, green, and purple, respectively.
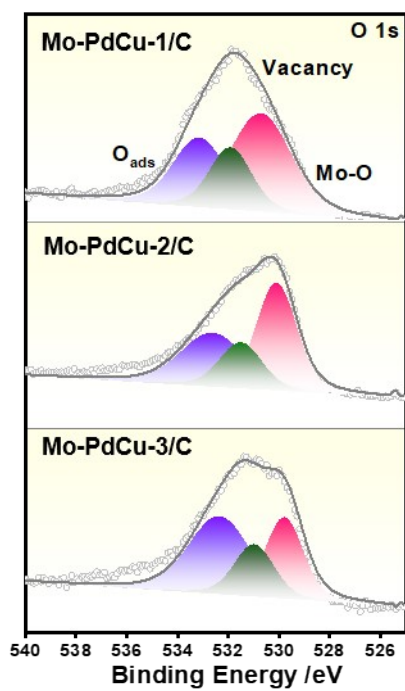
Figure S15. O 1s XPS patterns of Mo-PdCu-1/C, Mo-PdCu-2/C, and Mo-PdCu-3/C.
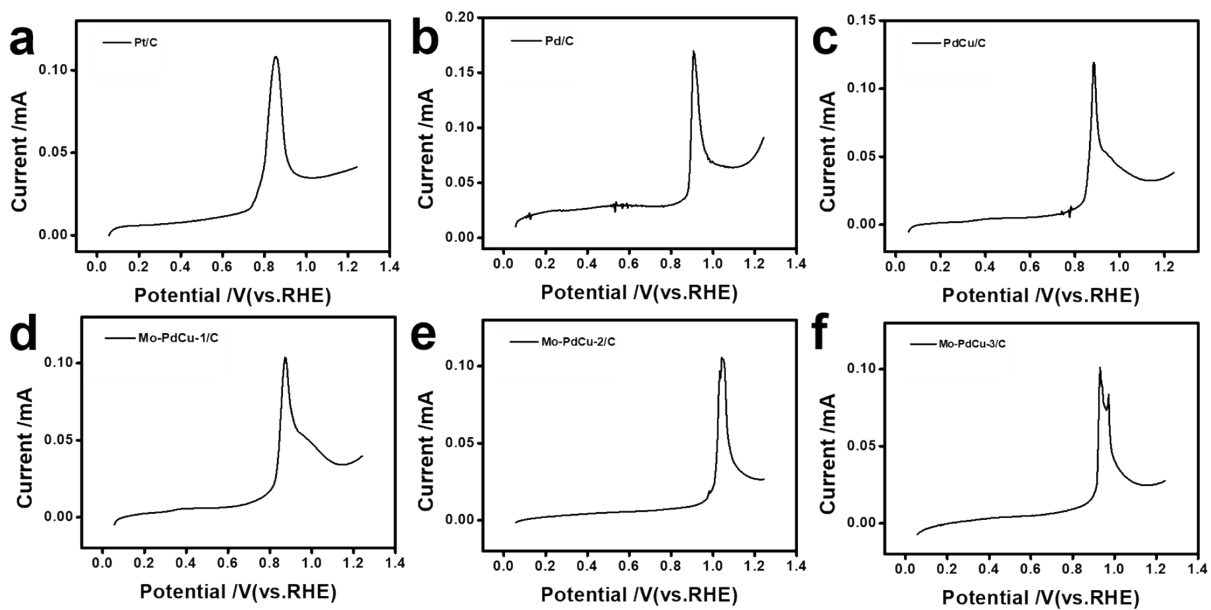
Figure S16. CO stripping curves in CO-saturated 0.1 M HClO$_4$ solution. (a) Pt/C, (b) Pd/C, (c) PdCu/C, (d) Mo-PdCu-1/C, (e) Mo-PdCu-2/C and (f) Mo-PdCu-3/C.
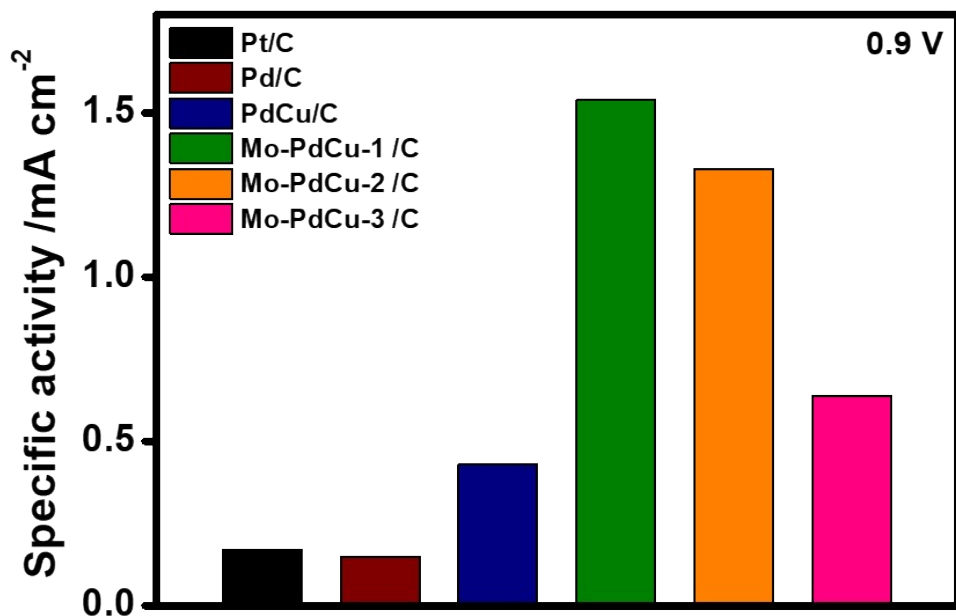
Figure S17. Specific activity of Pt/C, Pd/C, PdCu/C, Mo-PdCu-1/C, Mo-PdCu-2/C and Mo-PdCu-3/C.
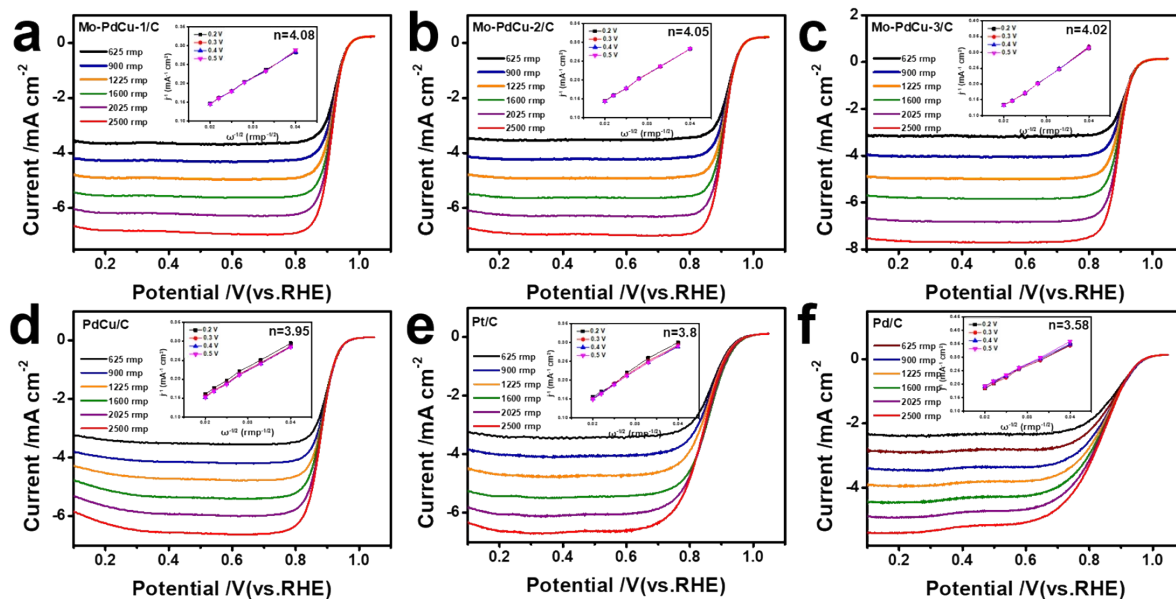
Figure S18. The rotating disk electrode plots of the catalysts. Spectrum of (a) Mo-PdCu-1/C, (b) Mo-PdCu-2/C, (c) Mo-PdCu-3/C, (d) PdCu/C, (e) Pt/C and (f) Pd/C in oxygen-saturated 0.1 M NaOH at rotation speeds ranging from 625 to 2,500 rpm and a scan rate of 10 mV s^{-1}; inset K-L curves.
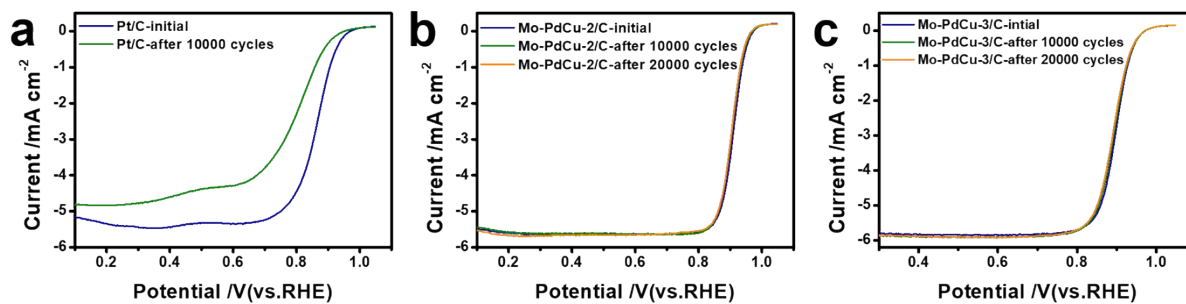
Figure S19. ORR stability of the catalyst. ORR polarization curves for (a) Pt/C, (b) Mo-PdCu-2/C, and (c) Mo-PdCu-3/C before and after cycles of ADT-O_2 in O_2-saturated 0.1 M NaOH solution.
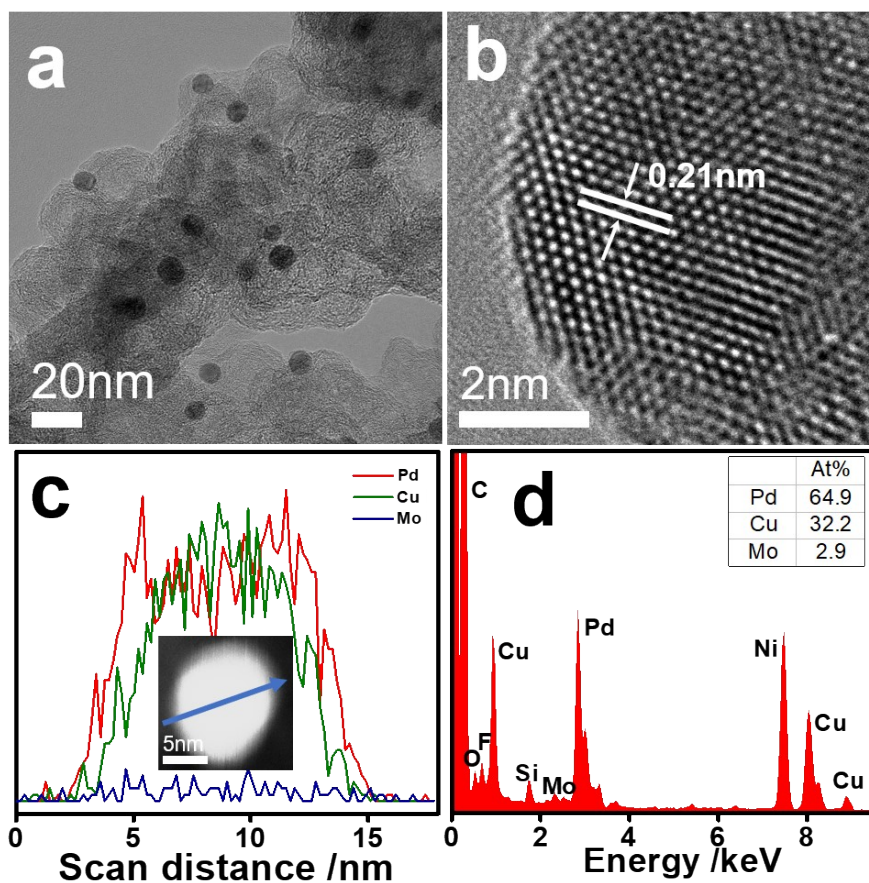
Figure S20. The morphology and element characterization of Mo-PdCu-1/C after stability test. (a) Representative TEM image, (b) HRTEM image, (c) HAADF-STEM-EDS elemental line scans, and (d) STEM-EDS pattern of Mo-PdCu-1/C after 20,000 cycles ADT-O_2 in O_2-saturated 0.1 M NaOH solution.
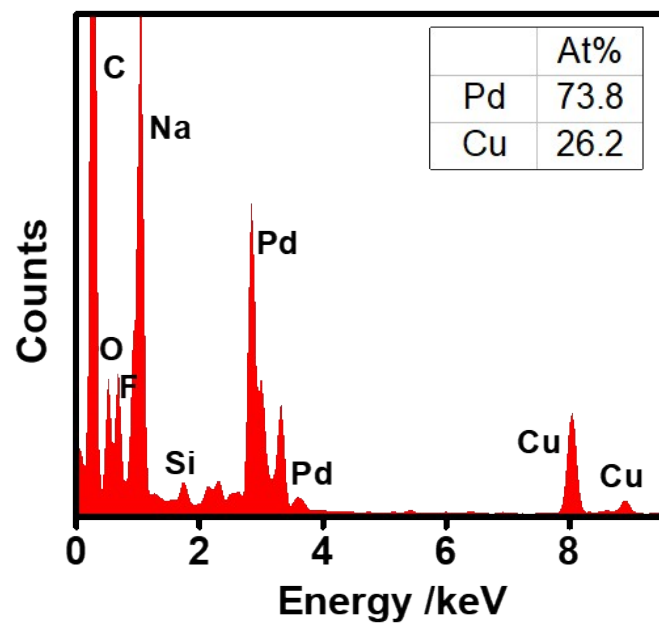
Figure S21. STEM-EDS pattern of PdCu/C after ORR 10000 cycles ADT-O_2 in O_2-saturated 0.1 M NaOH solution.

Figure S22. The TEM images of Pt/C and Pd/C after stability test. Representative TEM images of Pt/C and Pd/C (a, d) before and (c, f) after ORR 10,000 cycles ADT-O$_2$ in O$_2$-saturated 0.1 M NaOH solution.

2: Supplementary Table

Table S1. Summary of elemental percentages of different catalysts from EDS, XPS, and ICP.
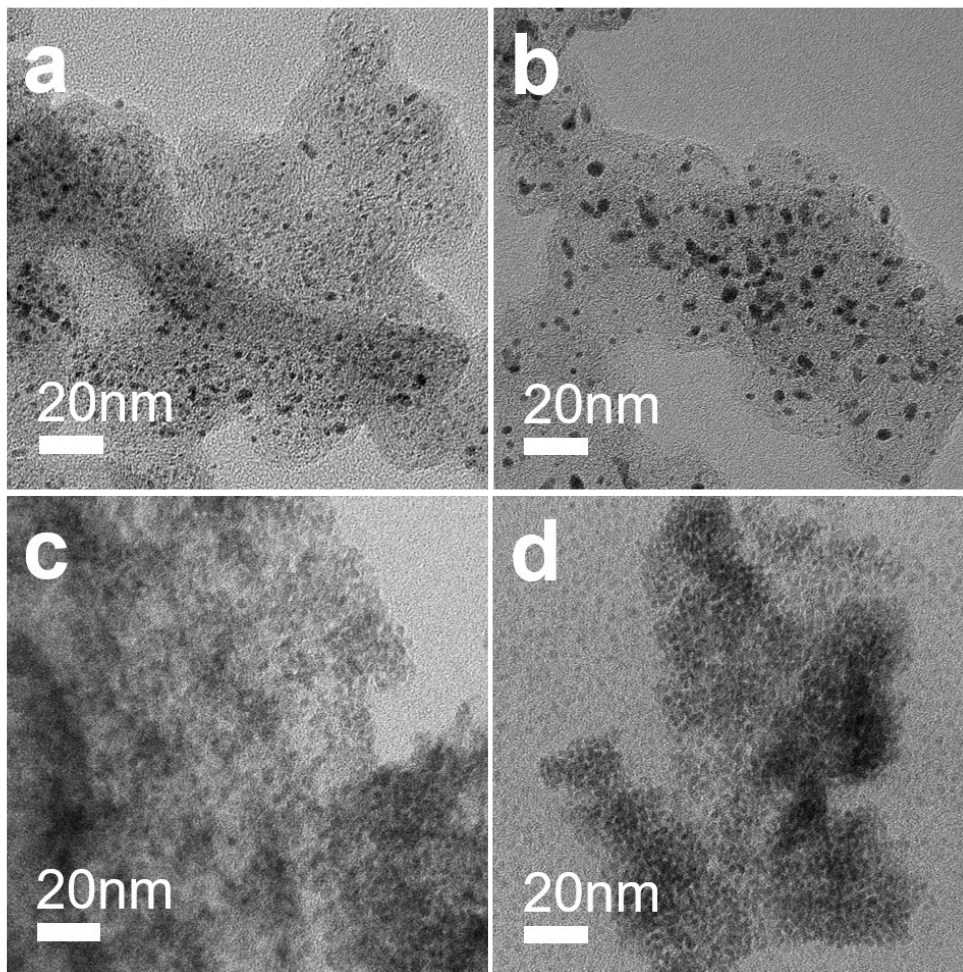
		Mo-PdCu-1/C	**Mo-PdCu-2/C**	**Mo-PdCu-3/C**	**PdCu/C**
EDS	Pd	57.7	50.4	41.9	54.9
	Cu	39.1	42.4	45.9	45.1
	Mo	3.2	8.2	12.2	
XPS	Pd	62.6	56.4	53.5	51.4
	Cu	29.1	33.3	32.4	48.6
	Mo	8.3	10.3	14.1	
ICP	Pd	41.9	35.5	37.7	48.2
	Cu	53.2	55.9	51.4	51.8
	Mo	4.9	8.6	10.9	

Table S2. Summary of elemental valence percentages of different catalysts from XPS.

		PdCu/C	Mo-PdCu-1/C	Mo-PdCu-2/C	Mo-PdCu-3/C
Pd	+2	53.34%	34.42%	40.90%	41.12%
	0	45.66%	65.58%	59.10%	58.88%
Cu	+2	45.00%	34.30%	37.81%	43.80%
	0	55.00%	65.70%	62.19%	56.20%
Mo	+6		85.00%	88.90%	92.84%
	+5		15.00%	11.10%	7.17%
O	Vacancy		21.48%	19.77%	18.37%
	Mo-O		48.83%	43.25%	33.62%
	O_{ads}		29.68%	36.98%	48.01%

Table S3. Summary of ECSA of different catalysts from CO stripping curve (Unit is m^{-2} g^{-1}_{Pd+Pt}).

	Pt/C	Pd/C	PdCu/C	Mo-PdCu-1/C	Mo-PdCu-2/C	Mo-PdCu-3/C
ECSA	69.49	59.07	54.85	78.19	62.24	58.32